Biomechanics of the movable pretarsal adhesive organ in ants and bees

Walter Federle*, Elizabeth L. Brainerd†, Thomas A. McMahon‡§, and Bert Hölldobler*¶

*Zoologie II, Biozentrum, Am Hubland, 97074 Würzburg, Germany; †Department of Biology, Morrill Science Center, University of Massachusetts, Amherst, MA 01003-5810; and ‡Division of Applied Sciences, Harvard University, Cambridge, MA 02138

Contributed by Bert Hölldobler, March 21, 2001

Hymenoptera attach to smooth surfaces with a flexible pad, the arolium, between the claws. Here we investigate its movement in Asian weaver ants (*Oecophylla smaragdina*) and honeybees (*Apis mellifera*).

When ants run upside down on a smooth surface, the arolium is unfolded and folded back with each step. Its extension is strictly coupled with the retraction of the claws. Experimental pull on the claw-flexor tendon revealed that the claw-flexor muscle not only retracts the claws, but also moves the arolium. The elicited arolium movement comprises (*i*) about a 90° rotation (extension) mediated by the interaction of the two rigid pretarsal sclerites arcus and manubrium and (*ii*) a lateral expansion and increase in volume. In severed legs of *O. smaragdina* ants, an increase in hemolymph pressure of 15 kPa was sufficient to inflate the arolium to its full size. Apart from being actively extended, an arolium in contact also can unfold passively when the leg is subject to a pull toward the body.

We propose a combined mechanical–hydraulic model for arolium movement: (*i*) the arolium is engaged by the action of the unguitractor, which mechanically extends the arolium; (*ii*) compression of the arolium gland reservoir pumps liquid into the arolium; (*iii*) arolia partly in contact with the surface are unfolded passively when the legs are pulled toward the body; and (*iv*) the arolium deflates and moves back to its default position by elastic recoil of the cuticle.

The capacity to hold on to smooth surfaces is essential for small animals that live on plants. Some insects can produce adhesive forces equivalent to more than 100 times their own body weight on perfectly smooth surfaces (e.g., refs. 1 and 2). However, these insects are able not only to hold on firmly, but also are able to run around swiftly on a smooth substrate. It is evident that, to master these different tasks, insects must have fast and effective control over their adhesive forces. However, almost nothing is known about the mechanisms of how insects control surface attachment and detachment. As a first step toward understanding the insects' control of adhesion, it is necessary to analyze how adhesive pads are moved. Only a few studies have addressed the movement of insect adhesive organs (3, 4), with conclusions that were based mainly on morphological results.

In Hymenoptera, the arolium is a smooth pad located between the claws. As in many other insects (e.g., refs. 5–8), its adhesion to smooth surfaces is mediated by a thin liquid film between the arolium and the surface (W.F., unpublished data). The arolium morphology has been investigated by light (e.g., refs. 3 and 9) and scanning electron microscopy (10–12). Despite these studies, it has remained unclear how the arolium is moved. The assumed mechanisms were either inflation by blood pressure (10, 11) or the action of the claw-flexor muscle (3), but none of these mechanisms had ever been examined experimentally. In this study, we combine direct observation of the arolium motion during walking with experimental tests of possible mechanisms.

Materials and Methods

Insects. We investigated workers of the Asian weaver ant, *Oecophylla smaragdina* and of the honeybee, *Apis mellifera*. Both species were selected because they have relatively large arolia that have been studied morphologically by previous authors (ref. 13 for *O. smaragdina* and refs. 3, 9, 10, and 12 for *A. mellifera*). Queenright *O. smaragdina* colonies were collected in West Malaysia and Brunei and kept in a laboratory nest (as described in ref. 14).

Morphology. We prepared semithin sections of the tarsus in *Apis* and *Oecophylla* workers. The tarsi were fixed in Carnoy's solution for 2 days and stored in 75% ethanol. They were dehydrated by washing in 100% ethanol (2 × 1 h). The specimens were immersed in propylene oxide for 2 × 20 min, stored for 12 h in a 1:1 solution of propylene oxide and epoxy embedding material (Epon)–Araldite mixture (15), and left in 100% Epon–Araldite mixture for 1 day. The resin was allowed to polymerize for 12 h at 60–75°C in a rubber mold. Blocks were sectioned serially at 1.5 μm by using glass knives and a microtome. Sections were attached to albuminized glass slides and stained with methylene blue at 60°C.

Intact or dissected tarsi were glued with double-sided tape onto SEM specimen holders, sputtered with gold for 5 min (25 mA), and investigated by using a Zeiss DSM 962 scanning electron microscope (working voltage 5–15 kV). "Live-action" SEM images of arolia were obtained by shock freezing *O. smaragdina* ants running on strips of smooth plastic. The insects were immersed rapidly in liquid Freon 22 at −150 to −160°C and dried overnight in a lyophilizer at −40°C (16). To avoid water condensation, the dried specimens were allowed to warm up slowly to room temperature inside a vacuum chamber.

High-Speed Video Observation. Insects were placed in a small rectangular plastic box covered on the lateral and upper sides with clean microscope slides. Ventral and lateral views of arolium attachments and detachments were recorded at 250 frames per sec with a Redlake (San Diego) PCI 1000 B/W high-speed video camera mounted on a dissecting microscope.

Arolium Inflation by Pressure. The middle legs of *O. smaragdina* were amputated and immersed in insect Ringer's solution (NaCl 10.4 g/liter/KCl 0.32 g/liter/$CaCl_2$ 0.48 g/liter/$NaHCO_4$ 0.32 g/liter). We cut off the leg in the middle of the tibia and left the leg in the Ringer's solution for 5 min to reduce hemolymph coagulation. The leg was dabbed dry with tissue and inserted with its cut-off end into the point of an injection needle. We sealed the leg in the needle by applying a droplet of fast-hardening acetone glue around the leg by using an insect pin. The injection needle was connected through tubing to a compressed-air tank with a valve and pressure regulator. Actual pressures

§Deceased February 14, 1999.

¶To whom reprint requests should be addressed at: Theodor-Boveri Institut für Biowissenschaften der Universität, Lehrstuhl für Zoologie II, University of Würzburg, D-97074 Würzburg, Germany. E-mail: bertholl@biozentrum.uni-wuerzburg.de.

The publication costs of this article were defrayed in part by page charge payment. This article must therefore be hereby marked "*advertisement*" in accordance with 18 U.S.C. §1734 solely to indicate this fact.

ECOLOGY

applied ranged from 0 to 50 kPa. The needle was fixed on the stage of a light microscope so that the arolium could be observed from the dorsal side. To prevent the arolium from drying out, the needle point was immersed in a small Petri dish containing Ringer's solution. Only when this treatment was applied did the arolium remain elastic long enough (>20 h) to perform several inflation/deflation cycles.

We measured the lateral width of the arolium. Starting from ambient pressure, we increased the pressure in steps of 2 kPa until full inflation was reached and decreased it back to zero. In the experiment shown in Fig. 3, two "rapid" and two "slow" inflation/deflation cycles were performed on the same arolium (pressure was changed every min or every 10 min, respectively).

Pull on the Claw-Flexor Tendon. *Apis* and *Oecophylla* legs were amputated and attached to the bottom of a transparent Petri dish by using melted paraffin. Only the proximal segments of the tarsus and the tibia were fixed so that the fifth tarsal segment and the pretarsus remained mobile. After the wax had hardened, Ringer's solution was added. Under a dissecting microscope, the cuticle of the tibia was opened to uncover the unguitractor apodeme. The preparation was transferred onto the stage of a light microscope. The unguitractor tendon was seized with fine forceps attached to a micromanipulator. Starting from the point where the first movements of the pretarsus became visible (defined as amplitude zero), the tendon was pulled in steps of 10 μm. When the maximum extension of the pretarsus was reached, we moved the apodeme back to the starting position, again in steps of 10 μm. During the pull on the unguitractor apodeme, lateral and ventral views of the pretarsus movements were recorded with a video camera attached to the microscope. To test the hydraulic-inflation hypothesis, the effect of puncturing the arolium was observed.

Passive Extension of Arolium. In workers of *A. mellifera* and *O. smaragdina*, tarsi of freshly amputated legs were attached to the point of a needle with a droplet of paraffin wax. With this method, legs could be seized without compressing them. The tarsi were pulled over a smooth microscope slide in such a way that the arolium just contacted the surface. The reaction of the arolium on pulls parallel to the surface was recorded with the high-speed video camera.

Results and Conclusions

Morphology. The major sclerites of the hymenopteran pretarsus can be seen in a sagittal section along with a whole mount of a honeybee middle-leg tarsus (Fig. 1 *B* and *C*). Our terminology follows that of Snodgrass (3). All sclerites are part of the exocuticle and are connected by cuticular membrane.

The arolium (ar) is a soft cuticular sac located between the claws. Its adhesive contact zone has a highly specialized fibrillar cuticle texture similar to the structure found in adhesive organs of other insect orders (Fig. 1*E*; see ref. 17). The arolium is supported by two hard pretarsal sclerites, arcus (ac) and manubrium (ma). The arcus is an endosclerite that has the form of a flat "U"-shaped band, which is embedded in a thin membrane (Fig. 1 *B–D* and *F–I*). Its bottom is attached to the ventral side of the arolium close to the planta (Fig. 1*B*). The arcus arms support the lateral walls of the arolium (Fig. 1*D*). The manubrium is hinged between the claws (Fig. 1*A*). It is a longitudinal sclerite on the dorsal side of the pretarsus.

As in other insects, the hymenopteran tarsus does not contain any intrinsic muscles. However, the long claw-flexor apodeme (ut) runs through the whole tarsus and reaches up distally to the large sclerotized unguitractor plate (up) on the ventral side of the pretarsus (Fig. 1*B*). This apodeme (which shall be called "unguitractor tendon" here) connects proximally to the tripartite retractor unguis muscle located in the tibia and the femur. The unguitractor plate is attached to the base of the claws through tendon-like elastic cuticle (ref. 18; Fig. 1 *C* and *E*). Contraction of the unguitractor muscle thus mediates a flexion of the claws, which are hinged dorsally on a projection of the fifth tarsomere. On its distal side, the unguitractor plate is attached to the weakly sclerotized hairy planta (pl), which connects to the arolium (Fig. 1 *B*, *C*, and *E*).

A large part of the fifth tarsal segment is occupied by the arolium gland (ag; Fig. 1*B*). The glandular epithelium represents the epidermis, thus the gland lumen forms a liquid space within the cuticle separate from the hemocoel (hc; ref. 19). The lumen connects with the interior of the arolium through a small opening between arcus and manubrium (Fig. 1 *B* and *F*). When punctured with microcapillaries, however, arolia leak droplets that coagulate, suggesting that the contained liquid is similar to hemolymph.

Movement of the Arolium. Fig. 2 *A–C* show typical high-speed video sequences of steps of ants and honeybees walking upside down on glass. As a rule, the claws touched the surface before the arolium (Fig. 2*A*). When a foot was put down, the claws first retracted until they reached a position perpendicular to the tarsus (Fig. 2*B*). The arolium then was unfolded and extended down to the surface. In *O. smaragdina*, we also observed an apparent, gradual increase in size, which suggests an inflation of the arolium. At the end of each step, the claws extended and the arolium deflated until it detached from the surface (Fig. 2*C*).

Arolium movement was coupled strongly with the movement of the claws. Extension of the arolium never occurred without a retraction of the claws. When the arolium unfolded, the unguitractor plate was always completely drawn back into the fifth tarsomere. When the foot detached, the unguitractor plate moved out of the fifth tarsomere so that it became fully or partly exposed.

Fig. 1*A* shows arolia of shock-frozen *O. smaragdina* ants in the retracted and the extended phases. The arolium movement is complex and can be described as (*i*) a rotation around a horizontal axis located near the distal end of the manubrium and as (*ii*) a lateral expansion of the organ in the extended phase and an invagination in the retracted phase.

In the retracted position of the arolium, the distal edges are folded up near the manubrium base so that this sclerite is partly hidden behind the folded arolium (Fig. 1*A Top*). When the arolium unfolds, these edges move down to the surface and the manubrium becomes exposed (Fig. 1*A Bottom*).

Arolium Inflation by Pressure. Fig. 3 shows the effect of hemolymph pressure on the size of the arolium in *O. smaragdina*. Pressure inflated the arolium to its maximal size. When the pressure was reduced again, the arolium deflated back to its original size. This behavior shows that arolium inflation is elastic and that deflation is driven by elastic recoil of the arolium cuticle. Most inflation-deflation curves showed a pronounced hysteresis so that intermediate arolium sizes were reached at higher pressures during inflation and at lower pressures during deflation. Hysteresis was weaker (but still present) when we waited for 10 min between each applied pressure change. The difference between slow and rapid inflation-deflation cycles indicates that pressure balance was reached only slowly. However, the observed hysteresis may also reflect viscoelastic properties of the arolium cuticle (17). In *O. smaragdina*, complete inflation was reached repeatedly at high pressures between 10 and 16 kPa (n = 10 slow inflations in 5 different legs).

Pull on the Claw-Flexor Tendon. We investigated movements of the pretarsus caused by a controlled pull on the unguitractor tendon. The unguitractor muscle not only retracted the claws but also

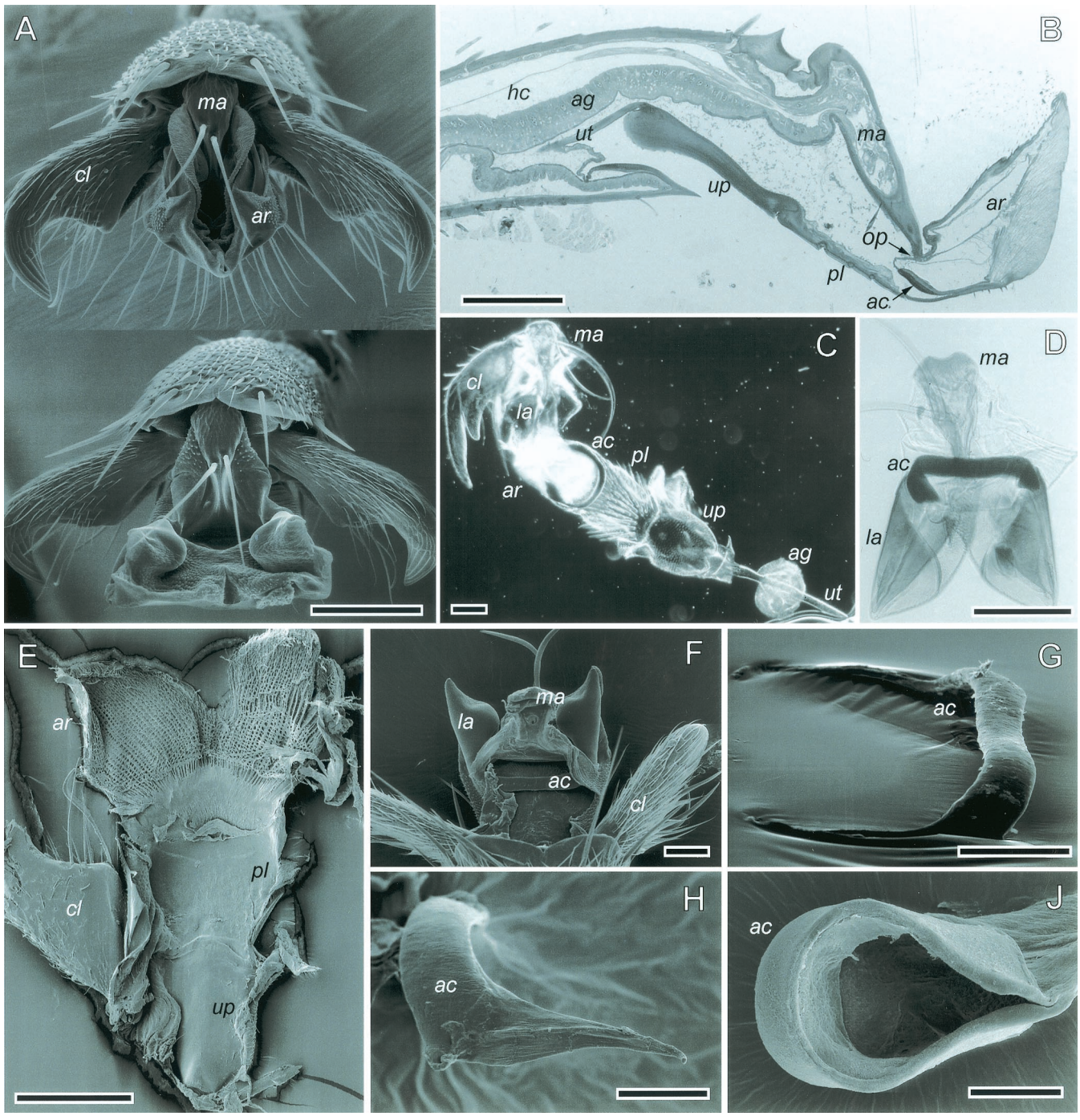

Fig. 1. (*A*) *O. smaragdina* arolium in the retracted (*Top*) and the extended phases (*Bottom*). (*B*) Sagittal section of a honeybee hind-leg pretarsus. (*C* and *D*) Whole mounts of pretarsi in *A. mellifera* and *O. smaragdina*, respectively. (*E*) *O. smaragdina*, inner view of ventral arolium cuticle. (*F*) *O. smaragdina*, dorsal view into opened arolium. (*G* and *H*) *O. smaragdina*, dissected arcus, lateral views. (*H*) Nonsclerotized arcus arm. (*I*) *A. mellifera*, dissected arcus with attached arolium cuticle. ac, arcus; ag, arolium gland; ar, arolium; cl, claw; hc, hemocoel; la, lateral arolium walls; ma, manubrium; pl, planta; up, unguitractor plate; ut, unguitractor tendon; op, opening. [Bars = 100 μm (*A–E*), 50 μm (*F*, *G*, and *I*), and 20 μm (*H*).]

moved and unfolded the arolium. Video sequences of pretarsal movements recorded during tendon-pull experiments in *O. smaragdina* are shown in Fig. 2*D* (lateral view) and Fig. 2*E* (ventral view). It can be seen that the elicited arolium movement in *O. smaragdina* was similar to that observed in freely walking animals because it consisted of a rotary motion and a lateral extension. A schematic model of the underlying mechanism is presented in Fig. 2*H*. When the unguitractor tendon was pulled, the unguitractor plate was drawn back into the 5th tarsomere. As the pretarsus is hinged on the dorsal front margin of the 5th tarsal segment ("unguifer"), the pull of the tendon makes the entire pretarsus (claws, manubrium, arolium, arcus, planta, and unguitractor plate) rotate around the unguifer joint (phases 1 to 2 in Fig. 2*H*). This rotation (clockwise in Fig. 2*H*) continues until the unguitractor plate hits the ventral, anterior margin of the 5th tarsal segment. In phase 2, claws and manubrium have almost reached their maximum flexion and the unguitractor plate is inclined relative to the direction of the tarsus. When the tendon

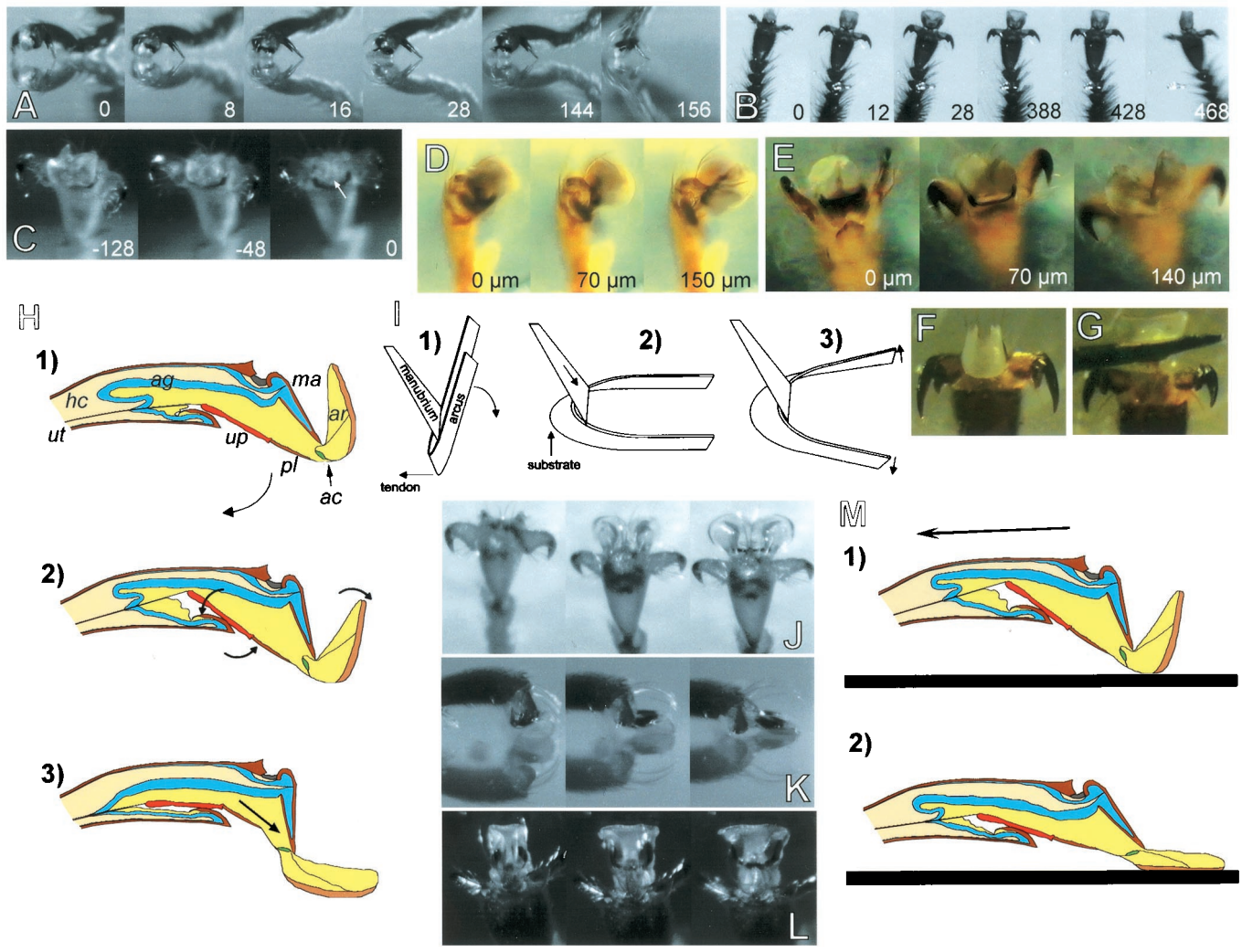

Fig. 2. (*A–C*) High-speed recordings of steps taken upside down on a glass plate (numbers indicate time in milliseconds). (*A*) *A. mellifera*, lateral view. (*B*) *A. mellifera*, ventral view. (*C*) *O. smaragdina*, arolium deflation before detachment (arrow indicates point of detachment). (*D* and *E*) *O. smaragdina*, experimental pull on the unguitractor tendon; numbers indicate the amplitude of the tendon pull (''0'' is defined as the tendon-pull amplitude where the first pretarsus movement was visible). (*D*) Pretarsus lateral view. (*E*) Ventral view, arolium surface focused. (*F*) *A. mellifera*, arolium at maximal pull of the tendon (200 μm). (*G*) Same as *F*, arolium spread laterally by application of upward pressure to the planta with an insect pin. (*H*) Model of arolium extension caused by the contraction of the claw-flexor muscle. For abbreviations see legend for Fig. 1. (*I*) Model of the interaction between the two arolium sclerites, arcus and manubrium. (*J–L*) Passive extension of arolium in contact with a glass surface. (*J*) *O. smaragdina*, pull of severed leg in the direction toward the body. (*K* and *L*) Pull of legs of freshly killed *A. mellifera* toward the body, lateral and frontal view of arolium, respectively. (*M*) Model of passive arolium extension caused by substratum contact and horizontal pull of the leg.

is pulled further (phases 2 to 3 in Fig. 2*H*), the unguitractor plate is not drawn further back into the tarsus, but it aligns to the direction of the pull by rotating around the anterior ventral margin of the 5th tarsomere (counterclockwise in Fig. 2*H*). As a consequence, the distal end of the planta and the attached U-shaped arcus are pushed upwards. A similar movement occurs when the arolium contacts the surface. The upward movement of the arcus base makes this U-shaped sclerite rotate around the distal end of the manubrium. The flexible connection of the arcus base to the ventral side of the pretarsus is the joint of this rotary motion (see Fig. 1*B*). Fig. 2*I* shows a model of the interaction between arcus and manubrium. The manubrium pushes down the lateral arms of the arcus so that the arolium is folded down. When observed in lateral view, the arcus arms with the attached lateral arolium walls move from a position approximately parallel to the manubrium (phase 1 in Fig. 2*H*) down to an extended position at an angle of about 100° to the manubrium (phase 3 in Fig. 2*H*).

Lateral Extension. The movement of the arolium consists not only of a rotation, but also of a lateral extension (Fig. 1*A* and Fig. 2 *B* and *C*). Our findings suggest that it can be explained by two different mechanisms, which have different importance in *A. mellifera* and *O. smaragdina*.

Arcus Movement. In *A. mellifera*, a pull on the claw-flexor tendon caused a rotation of the arolium but almost no lateral extension (Fig. 2*F* and Fig. 4). Only when an upward pressure to the planta was applied (as it occurs when the foot contacts the ground) did the arolium spread out conspicuously (Fig. 2*G*). The elastic lateral extension is mediated apparently by the flat U-shaped arcus. Destruction of this sclerite prevented a full lateral expansion. As a consequence of its particular geometry, the arcus can translate a vertical into a lateral movement (Fig. 2*I*). When the arolium is folded down to the surface, vertical pressure on the ventral base of the "U" elastically expands this sclerite in the lateral direction (Fig. 2*I*). Elasticity of the arcus probably resides in its nonsclerotized inner cuticle layer (Fig. 1*B*).

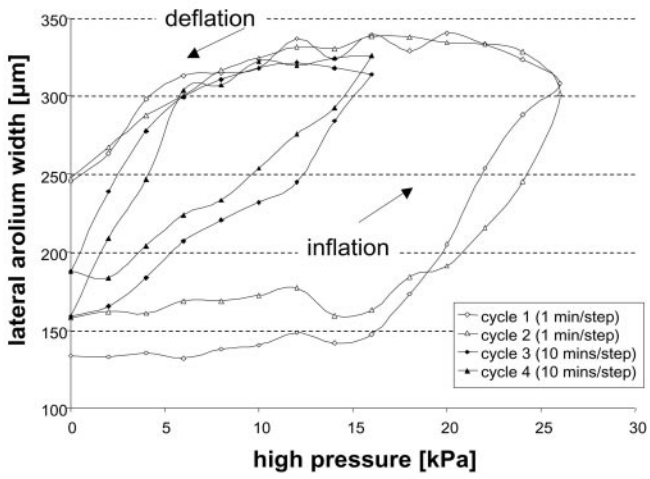

Fig. 3. Experimental arolium inflation and deflation by applied pressure in *O. smaragdina*.

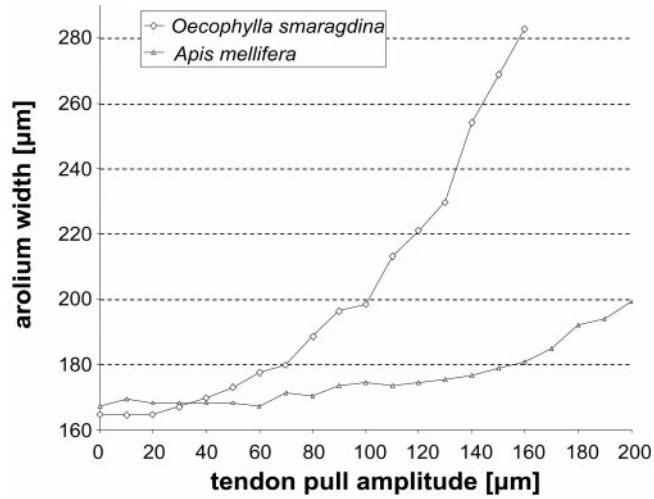

Fig. 4. Lateral arolium extension caused by experimental pull on the unguitractor tendon in *O. smaragdina* and *A. mellifera*.

Hydraulic Inflation. In *O. smaragdina*, the tendon pull alone spread the arolium to its full lateral width (Fig. 2*E*). As the morphology of the arcus in *O. smaragdina* strongly differs from *A. mellifera* (Fig. 1 *C* and *D* and *F–I*), a movement mechanism as shown in Fig. 2*I* is very unlikely. The sclerotized arcus base in *O. smaragdina* is almost straight and the lateral arms are very thin and not sclerotized (Fig. 1 *D*, *G*, and *H*). Lateral arolium expansion in this species seems to be caused by hydraulic inflation. At the maximal amplitude of the claw-flexor tendon pull, the arolium surface was curved strongly (Fig. 2*E*). When we punctured the arolium with a fine capillary, a pull on the tendon pressed out a small droplet and almost no lateral extension was visible.

We propose that the observed inflation can be explained by hydraulic compression of the arolium gland reservoir caused by the pretarsus movement itself. First, the backward movement of the unguitractor plate (phases 1 to 2 in Fig. 2*H*) creates a small air-filled pouch on the ventral side of the 5th tarsomere and thus compresses tarsal volume. However, visible inflation started only later in phase 2 (Fig. 2*H*), when the ventral side of the pretarsus hit the ventral, anterior margin of the 5th tarsal segment. Between phases 2 and 3 in Fig. 2*H*, the pretarsus is pressed against the ventral anterior end of the 5th tarsomere and the ventral side of the pretarsus gets indented at the transition between unguitractor plate and planta. Thus, pretarsal volume is compressed and liquid is forced forward into the arolium (phase 3 in Fig. 2*H*).

Passive Extension of Arolium. When we pulled live *O. smaragdina* ants or honeybees across a glass surface, the arolia of the legs opposite to the direction of the pull unfolded (Fig. 2 *J–L*). Even freshly killed insects responded with the extension of the arolium when a leg was pulled in the direction toward the body (see arrow in Fig. 2*M*). In *O. smaragdina* (but not in *A. mellifera*), this reaction was even operative in severed legs (Fig. 2*J*). Thus, it is not an active response but a passive reaction of the mechanical system to a pull on the leg. As in the active movement, the arolium extends and spreads out laterally. A hypothetical model of the underlying mechanism is shown in Fig. 2*M*. Because of its adhesive force, the arolium is pulled out of the tarsus. As a consequence, the manubrium gets extended and thus pushes the lateral arms of the arcus so that the arolium is folded down completely. The arolium folded back when the leg was moved in the distal direction.

Elastic Recoil. When the claw-flexor tendon was released, the pretarsus moved back to the extended position and the arolium folded up elastically. Elastic elements responsible for the countermovement of the pretarsus and arolium are present in several parts of the mechanical system. Resilin-like elastic cuticle at the unguifer acts as a claw-returning spring (18). Elasticity also resides in the arolium itself. Even an isolated preparation of arcus, manubrium, planta, and arolium preserved the full countermovement of the arolium. Amputation of the pretarsus distad to the unguitractor plate showed that the unguitractor plate alone still returned from the retracted to the original position. Only when we separated the plate laterally from its connecting membranes was elastic recoil finally lost.

Discussion

The adhesive pad in Hymenoptera is a flexible cuticular structure that can be actively moved and unfolded. Pretarsal attachment organs in many other insect orders are, by contrast, simply flexed together with the claws [e.g., the arolia in cockroaches (20, 21), stick insects (22), grasshoppers (23), or the hairy pulvilli in flies (5)]. Arolium extension in Hymenoptera also is mediated by the unguitractor muscle and thus coupled to the flexion of the claws. The organ bears an additional joint, however, formed by the two sclerites, arcus and manubrium. Arolia with arcus and manubrium also are found in members of the Trichoptera, Lepidoptera, and Mecoptera (24). A separate joint within the adhesive pad provides the possibility of employing the pad only if required. As the specialized cuticle of smooth adhesive pads is highly vulnerable to abrasion on rough surfaces (23), restricting its use to smooth surfaces is probably advantageous. Indeed, ants often make steps on rough or horizontal surfaces, in which the arolium is unfolded only partly or does not even touch the ground. The underlying control may reside partly in the mechanical system itself. Because arolium extension occurs later (at larger tendon-pull amplitudes) than the flexion of the claws (Fig. 2*A* and *B*), the movement is stopped when the claws interlock with a protrusion on the surface. Thus, the organ mainly unfolds on smooth surfaces, when the claws slip and find no resistance. Moreover, when the claws are hooked on a rough surface, no passive extension of the arolium takes place.

Our results indicate that the arolium movement can be described as a rotation and lateral expansion combined with a hydraulic pump mechanism. Inflation of adhesive pads has been reported from Thysanoptera (4). Heming (4) suggested that increased hemolymph pressure is generated by a compression of the abdomen. A more localized pump mechanism, as proposed here, is probably more appropriate to allow the insect to walk. However, we cannot rule out that leg circulatory organs (25, 26) also contribute to the inflation of the arolium.

The different arcus morphology in *A. mellifera* and *O. smaragdina* has apparent mechanical implications. The arolium of *O. smaragdina* unfolded more easily in the tendon-pull and passive-extension experiments. The strongly sclerotized arcus arms in *A. mellifera* are probably more resistant to a lateral expansion than the nonsclerotized thin arms in *O. smaragdina.* Higher stability of the extended arolium in *O. smaragdina* may be related to the particular nest-building behavior in this ant genus. Weaver ants draw leaves together and bind them with larval silk. As a rule, the legs of these forcefully pulling workers are attached with extended arolia onto the smooth upper surface of a leaf. Such living "clamps" can remain motionless for several hours (27).

The pretarsus of hymenopteran species is a striking example of a peripheral structure that features complex mechanical design but works with relatively simple central control. Pretarsal movements in all insects are mediated only by a single muscle that has no antagonist (28, 29). Purely mechanical control in the body periphery, as opposed to more centralized neuronal feedback, offers high reliability and shorter reaction times with a minimum expenditure of neuronal circuitry (30–33). Some tree-living tropical ants running on smooth twigs cannot be detached even by falling raindrops that are many times larger than the ants' bodies. This astounding capacity may be because of the passive extension of the arolium, which occurs almost simultaneously to the perturbation and is probably faster than reflex.

We are grateful to M. Obermaier (Zoologie II, Würzburg, Germany) who prepared semithin sections of *A. mellifera* and to G. Krohne who provided valuable help for the shock-freezing technique. M. Kiang and E. Chan collected preliminary data for this project. We thank S. Gorb and L. Frantsevich for helpful discussions. This work was supported by grants from the Deutsche Forschungsgemeinschaft (SFB 251) and the Karl von Frisch-Preis of the German Zoological Society (to B.H.).

1. Eisner, T. & Aneshansley, D. J. (2000) *Proc. Natl. Acad. Sci. USA* **97,** 6568–6573.
2. Federle, W., Rohrseitz, K. & Hölldobler, B. (2000) *J. Exp. Biol.* **203,** 505–512.
3. Snodgrass, R. E. (1956) *Anatomy of the Honey Bee* (Cornell Univ. Press, Ithaca, NY).
4. Heming, B. S. (1971) *Can. J. Zool.* **49,** 91–108.
5. Walker, G., Yue, A. B. & Ratcliffe, J. (1985) *J. Zool.* **205,** 297–307.
6. Ishii, S. (1987) *Appl. Entomol. Zool.* **22,** 222–228.
7. Lees, A. D. & Hardie, J. (1988) *J. Exp. Biol.* **136,** 209–228.
8. Jiao, Y., Gorb, S. & Scherge, M. (2000) *J. Exp. Biol.* **203,** 1887–1895.
9. Arnhart, L. (1923) *Arch. Bienenkd.* **5,** 37–86.
10. Conde-Boytel, R., Erickson, E. H. & Carlson, S. D. (1989) *Int. J. Insect Morphol. Embryol.* **18,** 59–70.
11. Pouvreau, A. (1991) *Can. J. Zool.* **69,** 866–872.
12. Lensky, Y., Cassier, P., Finkel, A., Teeshbee, A., Schlesinger, R., Delorme-Joulie, C. & Levinsohn, M. (1984) *Ann. Sci. Nat. Zool.* **6,** 167–175.
13. Wojtusiak, J., Godzínska, E. J. & Dejean, A. (1995) *Trop. Zool.* **8,** 309–318.
14. Hölldobler, B. (1979) *Z. Tierpsych.* **51,** 201–213.
15. Mollenhauer, H. H. (1964) *Stain Technol.* **39,** 111–114.
16. Eisner, T. & Eisner, M. (1989) *Bull. Entom. Soc. Am.* **35,** 9–11.
17. Gorb, S., Jiao, Y. & Scherge, M. (2000) *J. Comp. Physiol. A* **186,** 821–831.
18. Gorb, S. N. (1996) *J. Morphol.* **230,** 219–230.
19. Lensky, Y., Cassier, P., Finkel, A., Delorme-Joulie, C. & Levinsohn, M. (1985) *Cell Tissue Res.* **240,** 153–158.
20. Arnold, J. W. (1974) *Int. J. Insect Morphol. Embryol.* **3,** 317–334.
21. Frazier, S. F., Larsen, G. S., Neff, D., Quimby, L., Carney, M., DiCaprio, R. A. & Zill, S. N. (1999) *J. Comp. Physiol. A* **185,** 157–172.
22. Walther, C. (1969) *Z. Vergl. Physiol.* **62,** 421–460.
23. Slifer, E. H. (1950) *Ann. Entomol. Soc. Am.* **43,** 173–188.
24. Holway, R. T. (1935) *Psyche* **42,** 1–24.
25. Hantschk, A. M. (1991) *Int. J. Insect Morphol. Embryol.* **20,** 259–274.
26. Hustert, R. (1999) *Int. J. Insect Morphol. Embryol.* **28,** 91–96.
27. Hölldobler, B. & Wilson, E. O. (1990) *The Ants* (Belknap Press, Cambridge, MA).
28. Radnikow, G. & Bässler, U. (1991) *J. Exp. Biol.* **157,** 87–99.
29. Snodgrass, R. E. (1935) *Principles of Insect Morphology* (McGraw–Hill, New York).
30. Dickinson, M. H., Farley, C. T., Full, R. J., Koehl, M. A. R., Kram, R. & Lehman, S. (2000) *Science* **288,** 100–106.
31. Cruse, H., Brunn, D. E., Bartling, C., Dean, J., Dreifert, M., Kindermann, T. & Schmitz, J. (1995) *Adapt. Behav.* **3,** 385–418.
32. Full, R. J. & Koditschek, D. E. (1999) *J. Exp. Biol.* **202,** 3325–3332.
33. Kubow, T. M. & Full, R. J. (1999) *Philos. Trans. R. Soc. London B* **354,** 849–861.